Journal of Medical and Scientific Research

JMSR
www.jmsronline.com

Aishwarya S et al. J Med Sci Res. 2025; 13(3):277-285
DOI: http://dx.doi.org/10.17727/JMSR.2025/13-49

ORIGINAL RESEARCH OPEN ACCESS

Gastrointestinal stromal tumours: A clinicopathological perspective

Aishwarya S[1*], Shanmugapriya M[1], Suresh R[1], Eswari V[1], Aruthra P[1] and Lokeshwari V[1]

[1]Department of Pathology, Meenakshi Medical College Hospital and Research Institute, Meenakshi Academy of Higher Education and Research (Deemed to be University), Kanchipuram - 631552, Tamil Nadu, India

Abstract

Gastrointestinal stromal tumours (GIST) account for only 1-2% of all gastrointestinal (GI) neoplasms, yet they are the most common mesenchymal tumours of the GI tract. They arise from the interstitial cells of Cajal involved in gut motility and peristaltic movement. Early events in GIST development are activating mutations in CD117/c-KIT (cytoplasmic tyrosine kinase) or PDGFRA (Platelet Derived Growth Factor Receptor Alpha), which occur in most GISTs and encode for mutated tyrosine receptor kinases that are therapeutic targets for tyrosine kinase inhibitors. A small minority of GISTs possessing neither KIT nor PDGFRA mutations may have germline mutations in succinate dehydrogenase enzyme (SDH), suggesting a potential role of SDH in the pathogenesis. Immunohistochemical detection of c-KIT, DOG1 has proven to be highly sensitive and specific in the diagnosis of GISTs. Since accurate diagnosis by pathologists is crucial for current and future therapy, it is important to recognize KIT-negative GISTs, GISTs in specific clinical conditions, GISTs with unusual morphology, and GISTs with differential immunostaining that signify mutational subtypes. This case series highlights the biology, clinical presentations, morphology, immunohistochemistry, molecular analysis, and risk assessment of GISTs.

Keywords: GIST; CD117; c-KIT; PDGFRA mutation; immunohistochemistry; tyrosine kinase inhibitor; DOG-1; abdominal mass

Introduction

Gastrointestinal stromal tumours (GIST) represent the most common mesenchymal neoplasms of the gastrointestinal tract even though they account for only 1–2% of all GI malignancies. They arise from the interstitial cells of Cajal in the myenteric plexus, which regulate gut motility and peristalsis [1]. GISTs are typically characterized by activating mutations in the CD117/c-KIT (cytoplasmic tyrosine kinase) or PDGFRA (Platelet Derived Growth Factor Receptor Alpha) genes. The pathological diagnosis of GIST is complex and requires a combination of histological evaluation, immunohistochemistry, and increasingly, molecular testing [2].

In the gastrointestinal tract, gastric location is the most frequent (55.6%) followed by small bowel, colorectum and various other locations [3]. Rarely, extra gastrointestinal GISTs are seen arising from omentum, mesentery, retroperitoneum or pleura [4-6].

This study presents a spectrum of GISTs encountered in our institution, highlighting their diverse histopathological appearances, immunohistochemical profiles, and relevant molecular findings. By detailing these varied presentations, we aim to emphasize the diagnostic challenges and pathological nuances associated with GIST, as well as underscore the importance of integrated diagnostic approaches in guiding clinical management.

***Corresponding author:** Dr. Aishwarya S, MD, Associate Professor, Meenakshi Medical College Hospital and Research Institute, Meenakshi Academy of Higher Education and Research (Deemed to be University), Kanchipuram - 631552, Tamil Nadu, India. Email: aishwarya@mmchri.ac.in

Received 14 April 2025; *Revised* 9 June 2025; *Accepted* 16 June 2025; *Published* 25 June 2025

Citation: Aishwarya S, Shanmugapriya M, Suresh R, Eswari V, Aruthra P, Lokeshwari V. Gastrointestinal stromal tumours: A clinicopathological perspective. J Med Sci Res. 2025; 13(3):277-285. DOI: http://dx.doi.org/10.17727/JMSR.2025/13-49

Materials and methods

Study design and patient selection

This was a retrospective observational study conducted in the Department of Pathology at Meenakshi Medical College and Research Institute, Kanchipuram, Tamil Nadu. The study included 5 cases of Gastrointestinal Stromal Tumours (GISTs) diagnosed between March 2024 and February 2025. Detailed clinical information for all cases was taken from the patient's medical records.

Tissue processing and histopathological examination

Formalin-fixed, paraffin-embedded tissue sections were routinely processed. Haematoxylin and Eosin (H&E) stained sections were examined to evaluate morphological features including growth pattern, cellularity, nuclear pleomorphism, and mitotic figures, which were counted per 50 high-power fields (HPF). Risk stratification was performed according to established criteria.

Immunohistochemistry (IHC)

IHC staining was performed on 5 µm-thick sections mounted on poly-L-lysine coated slides. A non-biotin, micro-polymer based conjugate immune-peroxidase method was used. Heat-induced antigen retrieval was performed using Tris buffer with heat-induced antigen retrieval in a microwave. All cases were routinely stained with primary antibodies against CD117 and DOG1. In a specific case requiring further characterization, additional IHC markers including CD45, Pancytokeratin, S100, Synaptophysin, Chromogranin A, and Melan A were employed for differential diagnosis. Diaminobenzidine (DAB) was used as the chromogen, followed by counterstaining with Mayer's haematoxylin. Appropriate positive and negative controls were included in each run.

Interpretation of Immunohistochemistry:

Immunoreactivity was assessed based on both the percentage of positive cells and the intensity of staining. CD117 and DOG1 demonstrated membranous and cytoplasmic staining patterns.

Results

Case 1

A 60-year-old postmenopausal woman initially presented with lower abdominal pain and fever for 20 days. Initial evaluation, including abdominal ultrasound and contrast-enhanced computed tomography (CECT), suggested a pelvic abscess. Local examination revealed a vague, firm mass in the suprapubic region with restricted intrinsic mobility. Colonoscopy was performed up to the cecum, revealing coffee-coloured fluid in the colon. Blood investigations demonstrated moderate anaemia and neutrophilic leucocytosis.

During laparotomy, a large jejunal mesenteric mass adherent to the bladder was identified. A resection anastomosis with 5 cm margins on either side was performed. Gross examination revealed a lobulated cystic tumour measuring 17 x 12 cm (Figure 1a). The cut surface showed a cystic cavity filled with brown haemorrhagic fluid, alongside a small solid area. Histopathological evaluation demonstrated normal overlying mucosa with a well-circumscribed, underlying spindle cell tumour in the submucosa (Figure 1b) The spindle cells were arranged in fascicles with abundant eosinophilic cytoplasm and elongated nuclei with fine chromatin. Areas of necrosis, inflammatory cell collections (Figure 1c), and increased mitotic activity (10-15 per 50 high-power fields) were noted (Figure 1d). Immunohistochemistry confirmed the diagnosis of GIST, showing strong positivity for CD117 and DOG1.

Case 2

A 70-year-old female presented with a three-month history of early satiety and abdominal fullness. Abdominal ultrasound revealed a 15 x 10 cm mass originating from the posterior surface along the greater curvature of the stomach. Endoscopic biopsy was performed, and histopathological examination of the linear soft tissue samples showed fascicles of spindled smooth muscle cells with eosinophilic cytoplasm and uniform, oval to elongated nuclei with scattered blood capillaries. A provisional diagnosis of a benign spindle cell lesion was made. Immunohistochemistry was performed and demonstrated positivity for CD117 and DOG1, while S100, smooth muscle actin and desmin were negative. This immunophenotype confirmed the diagnosis of GIST. Despite the diagnosis and recommended treatment, the patient declined immediate tumour resection and was subsequently lost to follow-up.

Case 3

A 60-year-old female presented with a one-month history of intermittent abdominal pain and mucous in the stools. Abdominal ultrasound revealed a large, mixed echogenic mass with cystic degeneration and peripheral vascularity, extending from the right hypochondrium to the right iliac fossa. Subsequent CECT of the abdomen suggested GIST originating from the greater curvature of the stomach with extra-gastrointestinal spread to the mesentery and pelvis. Esophagogastroduodenoscopy (EGD) revealed a hiatus hernia and a gastric mass, from which a biopsy was taken. The biopsy showed gastric mucosa with ulceration and chronic inflammation in the lamina propria, with a focal area demonstrating spindle cells exhibiting eosinophilic cytoplasm and oval to elongated nuclei.

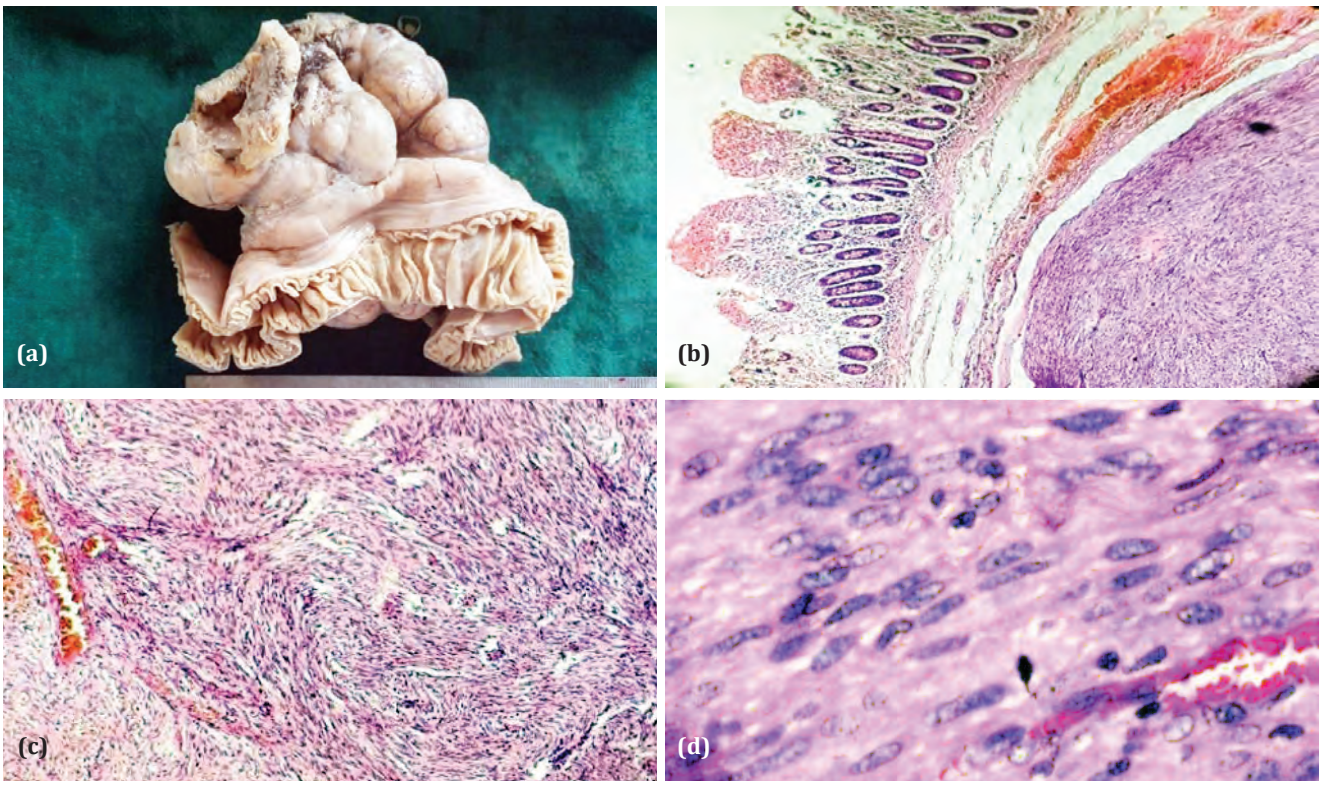

Figure 1: (a) Gross specimen showing lobulated cystic mass in the jejunum, (b) Hematoxylin and eosin (H&E) stained section, under 10x, showing normal mucosa at the left corner with the submucosal spindle cell tumour at the right corner, (c) H&E, under 10x, showing interlacing fascicles of spindle cells, (d) H&E, under 40x, showing spindled tumour cells with increased mitotic figures.

At laparotomy, multiple masses were observed in various locations, including the greater and lesser curvatures of the stomach, jejunum, ileum, transverse colon, pelvic colon, mesentery near the cecum, abdominal wall, and omentum. Specimens from these multifocal growths were submitted for histopathological examination. Grossly, the multiple nodular masses from the aforementioned gastrointestinal tract regions were predominantly solid with some cystic areas.

Microscopically, all masses displayed similar morphology: a well-circumscribed tumour composed of fascicles of spindle cells with eosinophilic cytoplasm and elongated, pleomorphic nuclei with prominent nucleoli. The tumour cells were seen centred around blood vessels. Focal nuclear palisading, cystic degeneration, and areas of haemorrhage were also noted. A brisk mitotic activity of 20 mitoses per 50 high-power fields was identified. Immunohistochemistry confirmed strong positivity for both CD117 /c-KIT and DOG1 in the tumour cells. Based on these findings, a diagnosis of multifocal GIST, spindled type, grade 2 (high grade), was given.

Case 4

A 49-year-old male presented to the emergency department with acute abdomen. CT scan revealed a distal jejunal tumour, necessitating emergency bowel resection and anastomosis. The resected specimen consisted of 55 cm length of jejunum with attached mesentery. Gross examination revealed a tan-coloured polypoidal mass measuring 6 x 4.5 x 2 cm, featuring a solid cut surface with multiple linear necrotic and ulcerated areas (Figure 2a,b). Two serosal nodules, each measuring 1 x 0.5 cm, were also identified, and 22 lymph nodes were dissected from the mesentery.

Microscopic examination of the jejunal mass demonstrated ulceration of the overlying mucosa with an underlying malignant tumour in the submucosa (Figure 2c). The tumour cells were round, arranged in solid sheets, with scant cytoplasm, vesicular nuclei with anisonucleosis, and prominent nucleoli. A very high mitotic rate of 80-90 mitotic figures per 50 HPF was observed (Figure 2d). Mature lymphocytes were interspersed within the tumour. No gland formation was noted. The tumour cells were seen infiltrating upto the serosa, and the necrotic and ulcerated areas also showed tumour infiltration. All 22 dissected lymph nodes showed normal histology.

The differential diagnosis for this undifferentiated submucosal small intestinal tumour included Non-Hodgkin's Lymphoma, Neuroendocrine tumour, GIST of Epithelioid type, and poorly differentiated carcinoma.

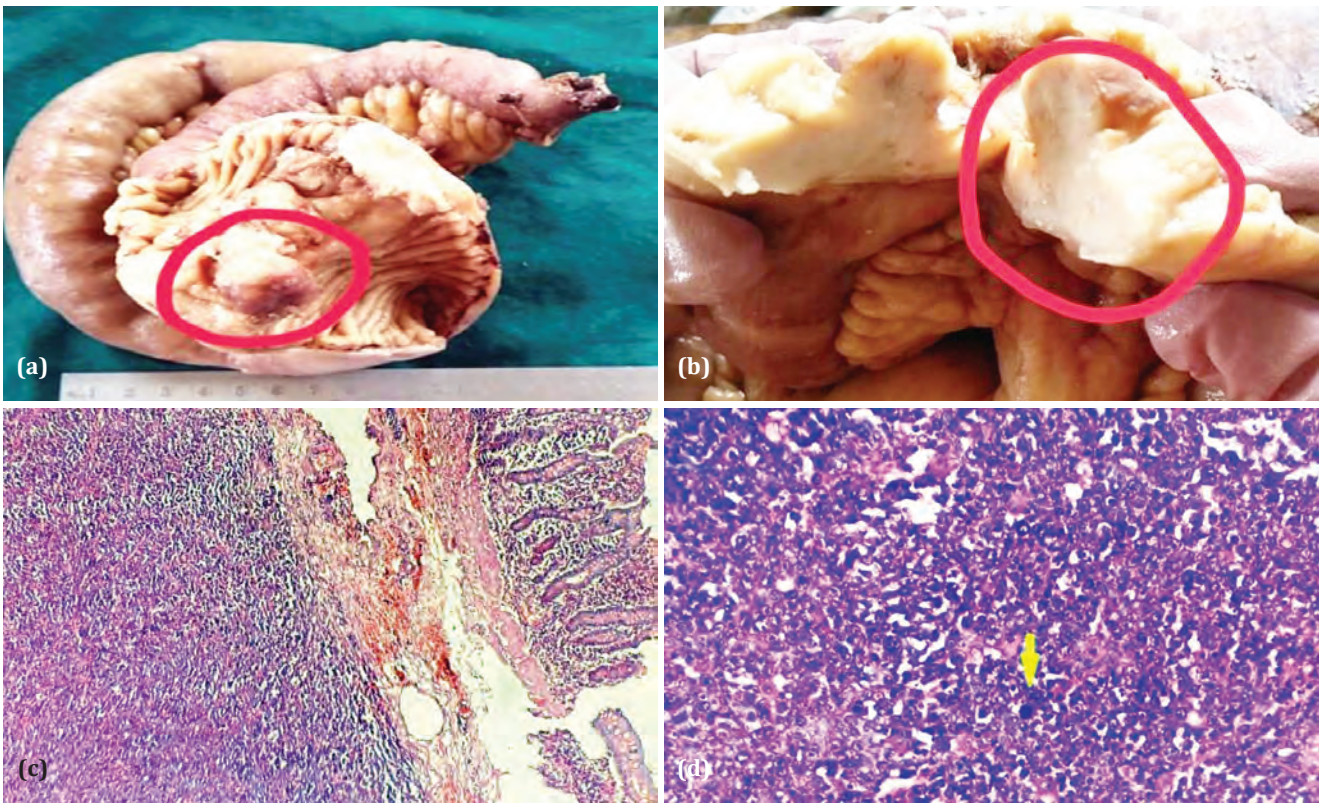

Figure 2: (a) Already cut open specimen of small bowel resection, distal jejunum with attached mesentery. Cut surface of small bowel showing tan coloured polypoidal mass, (b) Cut surface of the polypoid mass in small intestine showing solid grey white area, (c) H&E, under 4x, showing ulceration of the jejunal mucosa with an underlying malignant tumour in the submucosa, (d) H&E, under 40x, showing sheets of round cells with scant cytoplasm, vesicular nucleus with anisonucleosis and prominent nucleoli. Numerous mitotic figures were noted (80-90 mitoses per 50 high-power fields).

To establish the cell of origin, an immunohistochemical panel targeting these differential diagnoses was employed. The tumour cells were negative for CD3, CD20, synaptophysin, chromogranin, pancytokeratin, Melan A, and S100. However, CD45 was positive, with scattered positivity for CD117, and DOG1 was positive. Ki67 proliferation index was 60-70% (Figure 3). Based on the morphological features (epithelioid morphology) and immunohistochemical profile (positivity for CD45, scattered CD117, and DOG1), a diagnosis of epithelioid type, high-grade GIST, was given.

Case 5

A 63-year-old male was previously diagnosed with gastric GIST, characterized by positive CD117 and negative S100, vimentin, SMA and desmin on IHC. The initial tumour was deemed inoperable, leading to a 2-year course of Imatinib, which the patient subsequently discontinued. Upon recurrence, the patient presented with abdominal pain, distension, and inability to tolerate food, accompanied by loss of appetite and loss of weight. A palpable epigastric mass was noted, and a CECT scan revealed a large, lobulated exophytic gastric lesion with necrosis and calcification, adhering to the pancreas without infiltration. Multiple well-defined heterogeneously enhancing lesions suggestive of liver

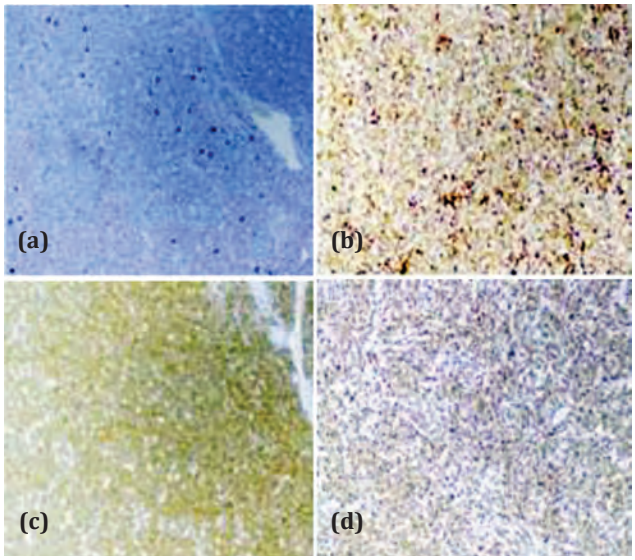

Figure 3: Immunohistochemistry (a) CD 117/c-KIT – scattered cells positive. (b) CD 45 – positive. (c) DOG 1- positive. (d) Ki 67 proliferation index – 60-70%.

metastasis were identified in segments III, V, VI, and VIII.

The patient underwent extensive surgery including total gastrectomy, distal pancreatico-splenectomy, left lateral segmentectomy of the liver, and non-anatomic

resection of right liver segments V and VII (Figure 4a). Grossly, cut surface of the stomach displayed multiple nodules, with the largest measuring 15x9.3x5.5cm, and the liver segments showed multiple grey-white nodules (Figure 4b). The spleen and pancreas appeared normal and 6 lymph nodes were resected.

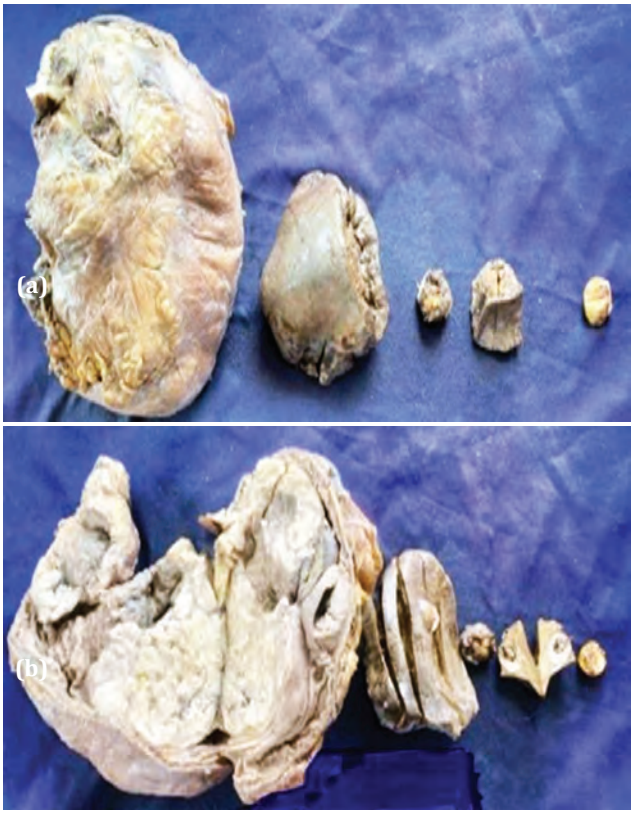

Figure 4: (a) Gross morphology of total gastrectomy, distal pancreas along with left total liver segmentectomy, right segments V, VII and a liver nodule, (b) Cut surfaces of the stomach and liver show multiple grey-white to grey-black nodular masses in the stomach and grey-white nodules in the liver.

Microscopically, the gastric masses showed a submucosal malignant neoplasm composed of spindle cells with eosinophilic cytoplasm, pleomorphic elongated nuclei, and inconspicuous nucleoli, arranged in intersecting fascicles. High mitotic count (10/50 high-power fields), scattered tumor giant cells, focal necrosis, and myxoid changes were seen (Figure 5a). The proximal margin was involved by the tumor (R1 resection), while the distal and radial margins were free. The spleen showed congestion but no tumor deposits, and the pancreas exhibited normal acini with tumor adherence but no invasion. The lymph nodes were free of tumor. Sections from liver segmentectomy, specifically segment V and segment VII showed multiple foci of tumor deposits (Figure 5b, Table 1).

Discussion

GISTs account for only 1- 3% of all GI neoplasms, yet

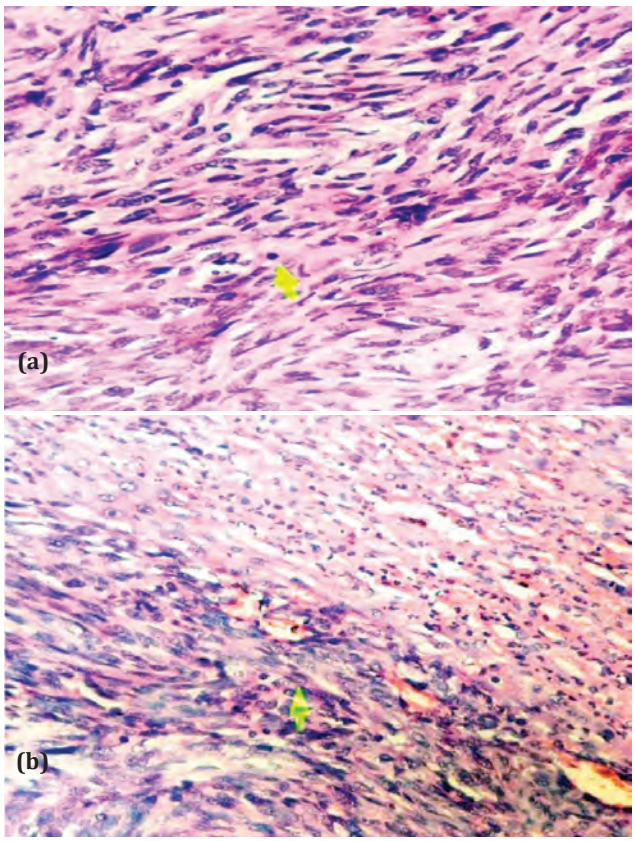

Figure 5: (a) Tumors cells showing eosinophilic cytoplasm, pleomorphic elongated nucleus, inconspicuous nucleoli and abundant mitosis, (b) Liver showing fascicles of spindle cells.

they are the most common mesenchymal tumours of the GI tract. Globally, the annual incidence of GIST is approximately 15 cases per million individuals per year [7]. GISTs are mostly seen in elderly population with a median age of 60 to 65 years. They are rare in children and young adults. When they occur in these age groups, they are associated with neurofibromatosis type 1 or as a part of Carney's triad [8, 9]. In our study, the mean age was 60 years. The youngest patient in our study was aged 49 and presented with distinct round cell morphology, was classified as high risk. Notably, this patient tested weakly positive for c-KIT. In contrast, all others exhibited spindle cell morphology and was c-KIT positive. Although gender distribution is generally equal, in our study 60% were females and 40% were males.

GISTs most commonly arise in the stomach accounting for approximately 60% of cases, but they can occur throughout the GI tract. The jejunum and ileum represent the second most frequent site (30%), followed by the duodenum (5%), colorectum (4%), and oesophagus or appendix (less than 1%) [10, 11]. Rarely, they can arise in the omentum, mesentery, or retroperitoneum, where they are referred to as extra gastrointestinal GIST [12-15]. Remarkably, primary GIST has also been reported in the pleura [16, 17]. In our study, 3 cases originated from stomach and 2 cases from jejunum.

Table 1: Summary of clinicopathological features of the cases under study.

Case no.	*Age/ Sex*	*Site*	*Primary symptom*	*Type of surgery*	*Histopathology*	*Mitosis*	*Tumour Grade*	*IHC analysis*	*Risk assessment*
1	60/F	Jejunum	Lower abdominal pain	Bowel resection and anastomosis	Spindle cell type	10-15/50 high power fields (HPF)	Grade 2 (High grade)	CD-117/c kit -positive DOG-1 positive	High risk
2	70/F	Stomach	Abdominal mass, early satiety	Endoscopic biopsy	Spindle cell type	2-3/50 HPF	Grade 2 (High grade)	CD-117/c kit -positive	Moderate risk
3	60/F	Stomach	Abdominal pain	Sleeve gastrectomy with ileal resection and anastomosis along with feeding jejunostomy	Spindle cell type	20/50 HPF	Grade 2 (High grade)	CD-117/c kit -positive	High risk
4	49/M	Jejunum	Acute Abdomen	Bowel resection and anastomosis	Round cell type Differential diagnosis: - Poorly differentiated carcinoma - Non-Hodgkin's lymphoma - Neuroendocrine tumor - GIST	80-90/50 HPF	Grade 2 (High grade)	CD-117/c kit-scattered cells positive CD45 positive DOG-1 positive Ki67 positive (60%-70%) Pan CK- negative S 100- negative Synaptophysin -negative Chromogranin A -negative Melan A-negative	High risk
5	63/M	Stomach with metastasis to liver.	Abdominal mass, loss of appetite and loss of weight	Total gastrectomy with distal pancreaticosplenectomy & right liver segmentectomy	Spindle cell type	10/50 HPF	Grade 2 (High grade)	CD-117/c kit -positive	High risk

Typically, GISTs are solitary, however, in rare cases, they may be multiple. Multiple GISTs refers to two or more GISTs within the GI tract involving one or more organs, without evidence of metastasis or recurrence. The diagnosis of multiple sporadic GISTs also require excluding familial GISTs, paediatric cases, or specific tumor syndromes such as NF1, Carney syndrome and Carney-Stratakis syndrome [18, 19]. In our study, one patient (case 3) presented with multiple growths from greater curvature, lesser curvature of stomach, jejunum, ileum, transverse colon, pelvic colon, mesentery near caecum, abdominal wall and omentum. Multiple nodular masses from all along the GI tract were predominantly solid with few cystic areas and showed spindled morphology. Case 5 presented with multiple nodular masses in the stomach, largest having the greatest dimension of 15cm and smallest, 3.5 cm. All the masses had a similar morphology of a well circumscribed tumor with fascicles of spindle cells. Both the above cases showed positive immunostaining for c-KIT and DOG 1 and both patients had no evidence of familial GISTs or tumor syndromes. This aligns with the diagnosis of multiple sporadic GISTs.

GISTs typically present as solid masses in the submucosa of the GI tract. But in rare cases, they can present as a lobulated, cystic mass. These cystic GISTs may contain areas of haemorrhage and necrosis leading to a complex appearance in imaging. It can be a diagnostic challenge, as they can mimic other conditions like ovarian cysts, pancreatic pseudocysts and mesenteric cysts [20]. In our study, a 60-year-old female presented with a lobulated cystic mass of 17x12 cm (Fig.1) in the jejunum. Its cut surface showed a cystic cavity filled

with brown haemorrhagic fluid along with a small solid area. All other cases appeared as nodular solid masses in the submucosa. This emphasizes the fact a lobulated cystic mass in the abdomen, when arising from the gastrointestinal tract, should raise suspicion for a cystic GIST.

Clinically, about 70% of GISTs present with non-specific symptoms that vary depending on tumour site and size. The most frequent symptoms are anemia, weight loss, gastrointestinal bleeding, abdominal pain and mass related symptoms. Patients may present with acute abdomen, obstruction, perforation or rupture and peritonitis [21, 22]. In our study, the clinical manifestations were lower abdominal pain, acute abdomen, abdominal mass, early satiety, loss of appetite and loss of weight. One patient in our study presented with a palpable suprapubic mass. Initial imaging studies, including USG and CECT, indicated a pelvic abscess and colonoscopy revealed brownish fluid in the colon. On surgical exploration, a large jejunal mesenteric mass adherent to the bladder was discovered, suggesting that this complex presentation, initially appearing as an infection, could be an atypical manifestation of GIST.

GISTs arise from interstitial cells of Cajal and is characterized by activating mutations in the c-KIT (CD117) and platelet derived growth factor receptor α (PDGFRA) protooncogenes in 85-95% of all cases [2]. The remaining 10–15% of cases lack aforementioned mutations and are referred as wild-type (WT) genotypes. Due to the different molecular drivers and distinct tumour biology, these neoplasms are highly resistant to tyrosine kinase inhibitor therapy and mandates a different treatment approach. GISTs arising in younger patients are much more commonly associated with the wild-type variant. In patients under 23 years of age, 85% of GISTs are WT [23]. These GISTs have shown defect in succinate dehydrogenase enzyme involved in Krebs cycle, either due to mutation or abnormal gene methylation and are referred as SDH-deficient GISTs [24]. Around 10% of wild type GISTs contain BRAF V600E mutation on exon 15, and the tumour is mostly seen in small intestine [25].

DOG1 (Discovered on GIST-1) gene that expresses a calcium-gated protein known as anoctinin-1 has been identified in 97% of all GISTs [26]. When used along with KIT, DOG1 has allowed up to 100% sensitivity in GIST detection and is highly specific for GISTs [27]. Numerous other receptors and markers such as CD34 (60–70%), smooth muscle actin (30–40%), S100 (5%), desmin (1–2%) and keratin (1–2%) have been found to be associated with GIST [28].

Microscopically, GISTs exhibit three primary morphological patterns. Most common is the spindle cell type, making up 70% of cases. These cells are elongated and arranged in short bundles or fascicles. The second type is the epithelioid cell type, comprising about 20% of GISTs and characterized by round or polygonal cells appearing in sheets or nests. The remaining 10% are classified as a mixed type, featuring both spindle and epithelioid cell morphology [29]. In our study, out of five cases analysed, four exhibited a typical spindle cell morphology. The remaining case displayed epithelioid morphology, characterized by round cells with a high mitotic count of 20-25 per 50 high-power fields and a significantly elevated Ki67 proliferation index, ranging from 60% to 70%. Immunohistochemical staining revealed scattered positivity for c-KIT and positivity for CD45 in this specific case. Vitiello et al, carried out RNA sequencing of GISTs from 75 patients, to study the differential immune profiles that distinguish the mutational subtypes of GIST. The study revealed that PDGFRA-mutant GISTs possess a distinct and more robust immune profile compared to KIT-mutant GISTs, characterized by significantly greater infiltration of immune cells. Immunohistochemical staining demonstrated that PDGFRA-mutant GISTs had a higher density of CD45+ leukocytes and CD8+ cytotoxic T cells, particularly clustered around perivascular structures, than their KIT-mutant counterparts. Quantitative analysis confirmed that even the most immune-infiltrated KIT-mutant GISTs exhibited fewer CD45+ and CD8+ cells per ×20 high-power field than PDGFRA-mutant tumors. Flow cytometric data corroborated these findings, showing significantly elevated CD45+ immune cell populations in PDGFRA-mutant GISTs. These results combined with the observed features, strongly suggests a probable *PDGFRA* mutation in this specific case [30].

The above findings are consistent with the understanding that epithelioid GISTs with high proliferation rates and CD45 expression are often associated with *PDGFRA* mutations, distinguishing them from the more common c-KIT-driven GISTs which typically present with spindle cell morphology. These results also suggest that PDGFRA-mutant GISTs that harbour a more cytologically active immune microenvironment, might have greater implications for immunotherapeutic responsiveness [30].

Risk stratification for primary GISTs is based on the AFIP criteria developed by Miettinen et al, which takes into account tumour size, mitotic rate, and tumour location classifying tumours into risk groups similar to the NIH system (Table 2) [31]. Modified NIH Criteria or the Joensuu Criteria is a modification of the NIH criteria

that incorporates tumour location and the presence of tumour rupture as additional high-risk factors (Table 3) [32]. It is evident that small intestinal GISTs show a markedly worse prognosis than gastric GISTs. In our study, one case fell under moderate risk and all the remaining cases posed high risk of recurrence. Among the high-risk cases, one patient manifested with synchronous liver metastases. Patients who underwent surgical resection of both primary and metastatic tumours, especially when combined with targeted therapies, have a significantly improved long-term survival, with some studies reporting 5-year survival rates up to 60% [33, 34,35].

Table 2: AFIP criteria – Risk assessment for recurrence and metastasis of Gastrointestinal stromal tumours.

Tumor parameters		*Risk of progressive disease# (%)*			
Mitotic rate	Size	Gastric	Duodenum	Jejunum/Ileum	Rectum
	≤2 cm	None (0%)	None (0%)	None (0%)	None (0%)
	>2 - ≤5 cm	Very low (1.9%)	Low (8.3%)	Low (4.3%)	Low (8.5%)
≤5 per 5 mm2	>5 - ≤10 cm	Low (3.6%)	(Insufficient data)	Moderate (24%)	(Insufficient data)
	>10 cm	Moderate (10%)	High (34%)	High (52%)	High (57%)
	≤2 cm	None##	(Insufficient data)	High##	High (54%)
	>2 - ≤5 cm	Moderate (16%)	High (50%)	High (73%)	High (52%)
>5 per 5 mm2	>5 - ≤10 cm	High (55%)	(Insufficient data)	High (85%)	(Insufficient data)
	>10 cm	High (86%)	High (86%)	High (90%)	High (71%)

Table 3: Modified NIH criteria (Joensuu's criteria) for risk assessment of Gastrointestinal stromal tumours.

Risk category	*Tumor size (cm)*	*Mitotic count (per 50 HPF)*	*Tumor site*	*Tumor rupture*
Very low risk	<2	<5	Any	Absent
Low risk	2-5	<5	Any	Absent
Intermediate risk	<5	6-10	Any	Absent
	5-10	<5	Gastric	Absent
High risk	>5	>5	Any	Absent
	>10	Any	Any	Absent
	Any	>10	Any	Absent
	Any	Any	Any	Present
	≤5	>5	Non-gastric	Absent
	5.1-10	≤5	Non-gastric	Absent

Conclusion

This case series highlights the diverse clinical, gross, microscopic, and immunophenotypic presentations of GISTs. The variations encountered, including gastric GIST with liver metastasis and jejunal GIST presenting as a round cell type with unusual immunophenotype underscore the diagnostic challenges associated with these tumours. The observation of a lobulated cystic tumour in the jejunum further emphasizes the morphological spectrum of GISTs and the need for a high index of suspicion. Our findings underscore the importance of detailed histopathology, immunohistochemistry, and clinical correlation in diagnosing and managing GISTs. Molecular characterization may provide further insights into prognosis and therapeutic strategies.

Conflict of interest

The authors declare no conflict of interest.

References

[1] Gupta SK, Rateria N. Gastrointestinal stromal tumors (GIST): an overview. Indian J Surg. 2021; 83:647–653.

[2] Niinuma T, Suzuki H, Sugai T. Molecular characterization and pathogenesis of gastrointestinal stromal tumor. Transl Gastroenterol Hepatol. 2018; 3:2.

[3] Søreide K, Sandvik OM, Søreide JA, Giljaca V, Jureckova A, et al. Global epidemiology of gastrointestinal stromal tumours (GIST): A systematic review. Cancer Epidemiol. 2016; 40:39–46.

[4] Toutounji Z, Alahmad Z, Attar M, Sarminy M, Alsado WM, et al. Unusual location of gastrointestinal stromal tumor (GIST): A case report. Int J Surg Case Rep. 2024; 119:109793.

[5] Arellano-Gutiérrez G, Martínez-Aldrete LF, Pérez-Fabián A, Maldonado-García EL. EGIST of the mesentery: Case report. Ann Med Surg (Lond). 2020; 60:480–483.

[6] Feng Y, Liu L. Characteristics and prognosis of retroperitoneal GISTs. Surg Endosc. 2025; 18:1–4.

[7] Gupta SK, Rateria N. Gastrointestinal stromal tumors (GIST): an overview. Indian J Surg. 2021; 83:647–653.

[8] Matyakhina L, Bei TA, McWhinney SR, Pasini B, Cameron S, et al. Genetics of Carney triad. J Clin Endocrinol Metab. 2007; 92:2938–2943.

[9] Mantalovas S, Karakousis VA, Sevva C, Roulia P, Savvakis S, et al. Multiple GISTs in NF1: A meta-analysis. Cancers (Basel). 2025; 17:1934.

[10] Miettinen M, Makhlouf H, Sobin LH. GISTs of the jejunum and ileum: 906-case study. Am J Surg Pathol. 2006; 30:477–489.

[11] Miettinen M, Sobin LH, Lasota J. GISTs of the stomach: 1765-case study. Am J Surg Pathol. 2005; 29:52–68.

[12] El Charif MH, Amro S, Boulos F, Khalife M, Shamseddine A, et al. Extra-GISTs: A misleading entity. Medicine (Baltimore). 2023; 102:33394.

[13] Alkhatib L, Albtoush O, Bataineh N, Gharaibeh K, Matalka I, et al. EGIST in the abdominal wall: Case report. Int J Surg Case Rep. 2011; 2:253–255.

[14] Miettinen M, Monihan JM, Rikala MS. GISTs in the omentum and mesentery. Am J Surg Pathol. 1999; 23:1109–1118.

[15] Miettinen M, Sobin LH, Lasota J. GISTs presenting as omental masses. Am J Surg Pathol. 2009; 33:1267–1275.

[16] Zhang CQ, Lu DG, Liu QF, Xiao W. Primary EGIST of the pleura: A case report. Oncol Lett. 2016; 11:3135–3138.

[17] Yi JH, Sim J, Park BB, Lee YY, Jung WS, et al. Primary EGIST of pleura: Case report. Jpn J Clin Oncol. 2013; 43:1269–1272.

[18] Kang DY, Park CK, Choi JS, Jin SY, Kim HJ, et al. Detection of multiple sporadic GISTs via PET/CT. Front Oncol. 2024; 14:1321179.

[19] Li C, Li W, Shang M, Wang P, Hu X. Dual-time PET/CT in sporadic GISTs. Front Oncol. 2024; 14:1321179.

[20] Chen L, Gu J, Zhang X, Yu A. Giant cystic ileal GIST with abscess. Front Surg. 2023; 9:1056831.

[21] Sorour MA, Kassem MI, Ghazal AA. GIST-related emergencies. Int J Surg. 2014; 12:269–280.

[22] Trupiano JK, Stewart RE, Misick C. Gastric stromal tumors: behavior correlation. Am J Surg Pathol. 2002; 26:705–714.

[23] Janeway KA, Liegl B, Harlow A. Pediatric KIT/PDGFRA WT GISTs. Cancer Res. 2007; 67:9084–9088.

[24] Ibrahim A, Chopra S. SDH-deficient GISTs. Arch Pathol Lab Med. 2020; 144:655–660.

[25] Huss S, Pasternack H, Ihle MA. BRAF mutations in WT GISTs. Hum Pathol. 2017; 62:206–214.

[26] Rasheed MW, Abiodun AE, Eziagu UB, Akinlawon A, Olori S, et al. IHC profile of GISTs in Nigeria. Ann Afr Med. 2023; 22:501–507.

[27] Lee CH, Liang C, Espinosa I. DOG1 utility in surgical pathology. Adv Anat Pathol. 2010; 17:222–232.

[28] Gama JM, Oliveira RC. Mesenchymal tumors beyond GIST. Gastrointest Disord. 2024; 6:257–291.

[29] Fülöp EM, Marcu S, Borda A, Moldovan C, Fülöp EF, et al. IHC features of GISTs. Rom J Morphol Embryol. 2011; 52:555–562.

[30] Vitiello GA, Bowler TG, Liu M. Immune profiles in GISTs. J Clin Invest. 2019; 129:1863–1877.

[31] Miettinen M, Lasota RJ. Pathology and prognosis of GISTs. Semin Diagn Pathol. 2006; 23:70–83.

[32] Rutkowski P, Bylina E, Wozniak A, Nowecki ZI, Osuch C, et al. Validation of Joensuu risk criteria. Eur J Surg Oncol. 2011; 37:890–896.

[33] Zhang HD, Yin XN, Mu MC, Chen HN, Cai ZL, et al. Prognostic factors for metastatic gastrointestinal stromal tumors treated with cytoreductive surgery: a retrospective cohort study. Scandinavian Journal of Gastroenterology. 2025; 12:1–1.

[34] Wang J, Wang T, Yang X. Surgery in GIST with liver metastases. Dig Liver Dis. 2023; 55:549–556.

[35] Shi YN, Li Y, Wang LP. GIST with liver metastases: 18-year experience. Medicine (Baltimore). 2017; 96:8240.